SCIENTIFIC REPORTS

OPEN

Premartensitic transition and relevant magnetic effects in $Ni_{50}Mn_{34}In_{15.5}Al_{0.5}$ alloy

Received: 21 January 2016
Accepted: 26 April 2016
Published: 16 May 2016

Yuqin Wu[1], Shaopu Guo[1], Shuyun Yu[2], Hui Cheng[3], Ruilong Wang[1,3], Haibo Xiao[1], Lingfang Xu[1], Rui Xiong[4], Yong Liu[4], Zhengcai Xia[3] & Changping Yang[1]

Resistance measurement, *in situ* optical microscopic observation, thermal and magnetic measurements have been carried out on $Ni_{50}Mn_{34}In_{15.5}Al_{0.5}$ alloy. The existence of a pronounced premartensitic transition prior to martensitic transition can be characterized by microstructure evolution as well as exothermic peak and smooth decrease of resistance and magnetization with obvious hysteresis over a wide temperature range upon cooling. Consequently, the alloy undergoes two successive magneto-structural transitions consisting of premartensitic and martensitic transitions. Magnetoelastic coupling between magnetic and structural degrees of freedom would be responsible for the appearance of premartensitic transition, as evinced by the distinct shift of transitions temperatures to lower temperature with external applied field of 50 kOe. The inverse premartensitic transition induced by magnetic field results in large magnetoresistance, and contributes to the enhanced inverse magnetocaloric effect through enlarging the peak value and temperature interval of magnetic entropy change ΔS_m.

Premartensitic state, referring to the intermediate state existing between the symmetric high temperature austenitic phase and a low-symmetry martensitic structure at low temperature, can be observed in the Ni-Mn-Ga ferromagnetic shape memory alloys[1–19]. The premartensitic phase shows approximately cubic symmetry with a micromodulated domain structure of parent phase, indicating the weak first-order nature of the premartensitic transition[2–5]. Anomaly of the elastic[2,6–9], thermal[2,9–12], resistivity[8,10,11,13–17], and magnetic properties[3,7–12,15–20] can be observed across this phase transition in Ni-Mn-Ga alloys. From the view of developing the application of Ni-Mn-Ga alloys, much effort has been devoted to research the origin of the premartensitic transition from parent phase to the intermediate state by theoretical and experimental methods. It is generally accepted that the premartensitic transition is a consequence of magnetoelastic coupling between the magnetic and structural degrees of freedom, as suggested by the strong magnetic field dependence of premartensitic transition temperature[3,8,9,11,13,16]. However, large magnetic effects associated with the premartensitic transition in Ni-Mn-Ga alloys have seldom been reported up to now due to the quite narrow temperature range and small magnetization change across the premartensitic transition. It would be attractive to obtain such behavior in material with strong magneto-structural coupling.

As a new type of ferromagnetic shape memory alloys (FSMAs), off-stoichiometric $Ni_{50}Mn_{25+x}Z_{25-x}$ (Z = In, Sn, Sb) Heusler alloys have received much attention since firstly reported by Sutou *et al.*[21]. Such alloys exhibit strong magnetoelastic coupling with large magnetization difference between the ferromagnetic high-temperature austenitic phase and weak magnetic low-temperature martensitic phase. As a result, the transition temperatures of these alloys decease considerably when applying high magnetic field. Consequently, a magnetic-field-induced inverse martensitic transition (MT) from martensite to austenite occurs when a magnetic field is applied at a constant temperature close to the austenitic transition start temperature (A_s). Associated with the field-induced inverse MT, a variety of interesting properties, such as magnetic shape memory effect[22], magnetocaloric effect[23–27], and

[1]Hubei Collaborative Innovation Center for Advanced Organic Chemical Materials, Hubei Key Laboratory of Ferro & Piezoelectric Materials and Devices, Faculty of Physics and Electronic Science, Hubei University, Wuhan 430062, People's Republic of China. [2]School of Physics, Shandong University, Jinan 250100, People's Republic of China. [3]Wuhan National High Magnetic Field Center & School of Physics, Huazhong University of Science and Technology, Wuhan 430074, People's Republic of China. [4]School of Physics and Technology, Wuhan University, Wuhan, 430072, People's Republic of China. Correspondence and requests for materials should be addressed to R.L.W. (email: wangrlnju@gmail.com) or Z.C.X. (email: xia9020@hust.edu.cn) or C.P.Y. (email: cpyang@hubu.edu.cn)

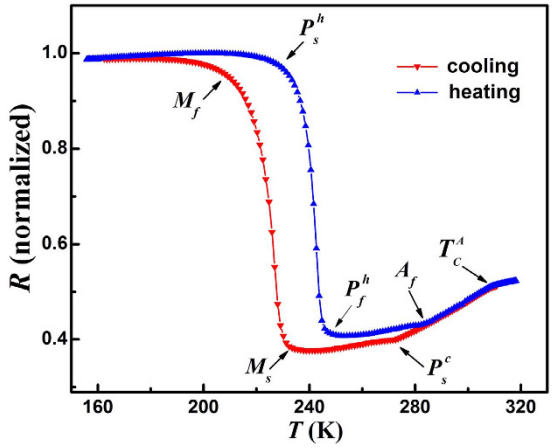

Figure 1. Temperature dependence of resistance $R(T)$ for $Ni_{50}Mn_{34}In_{15.5}Al_{0.5}$ alloy at zero field upon heating and cooling.

magnetoresistance[28,29] have been observed in the vicinity of the MT. However, there are few reports about the premartensitic transition in such Ga-free FSMAs. Recently, Ma *et al.* reported an intermediate phase transition prior to the martensitic transition and related magnetic properties, including magnetocaloric effect and magnetoresistance, in the high-pressure annealing $Ni_{43}Mn_{41}Co_5Sn_{11}$ alloy[30,31]. The intermediate phase transition can be evidenced by anomaly of magnetization and resistance upon heating, and the appearance of intermediate phase can be attributed to the enhancement of magnetoelastic coupling as the application of external pressure in fabrication process. Actually, chemical pressure can also be generated by relatively smaller atom substitution conveniently. Substituting the atoms in Ni–Mn–Z alloys by some smaller atom would be an effective method to get more pronounced intermediate phase or premartensitic transition behavior[25,26]. Since Al has the same valence electrons and smaller ionic radius compared to In, $Ni_{50}Mn_{34}In_{15.5}Al_{0.5}$ alloy formed by substituting In with Al was prepared. In this letter, two successive magneto-structural transitions with pronounced first-order nature, including MT and premartensitic transition, and related magnetic effects were reported.

Results

Figure 1 shows the temperature dependence of resistance R(T) curves for $Ni_{50}Mn_{34}In_{15.5}Al_{0.5}$ alloy. One can note that the resistance increases sharply at about 234 K upon cooling and decreases drastically at about 250 K upon heating, indicating the MT and reverse MT. Due to the first-order nature of the MT, a thermal hysteresis about 18 K appears. Compared with the parent $Ni_{50}Mn_{34}In_{16}$ alloy[28], the $Ni_{50}Mn_{34}In_{15.5}Al_{0.5}$ alloy exhibits MT at higher temperature due to the chemical pressure introduced by Al doping, as reported before[26,27]. A change in the slope of the resistivity at 310 K without hysteresis can be recognized as the second-order magnetic transition at Curie temperature of austenite (T_C^A). Another slope change at about 272 K, prior to MT, upon cooling with an obvious hysteresis (~14 K) can be recognized as premartensitic transition, just as reported in Ni-Mn-Ga alloys[8,10,11,13–16]. However, the premartensitic transition here appears somewhat different with those of Ni-Mn-Ga alloys, where the hysteresis are very weak and could be hardly detected. The characteristic temperatures of the reversible MT and premartensitic transition, referring to the temperatures of martensite start and finish, premartensite start upon cooling and heating, and austenite start, were marked as M_s, M_f, P_s^c, P_s^h, P_f^h and A_s in the figure respectively.

Since the *in situ* optical microscopic observation has been proved as a powerful method to study the microstructure evolution of samples with first-order phase transition[32,33], it was employed to further confirm the existence of the premartensite phase in $Ni_{50}Mn_{34}In_{15.5}Al_{0.5}$ alloy. The optical micrographs at representative temperatures upon cooling are shown in Fig. 2. The sample is in austenitic phase at 300 K, exhibiting smooth surface after polish. The relative rough surface in Fig. 2(a) is resulted from being etched by dilute nitric acid, which would be good for the observation of the premartensite phase. Between P_s^c and M_s, many tiny domains-like structures appear, and the domain density increases with decreasing temperature, as shown in Fig. 2(b–e). Similar results have been observed in $Ti_{50}Ni_{48}Fe_2$ alloy through *in situ* dark-field image observations using electron microscopy, where the domains have been identified as premartensitic domains as a result of structural modulation of parent phase[34–36]. Striped fold and scaly wrinkles appear after M_s and keep increasing at expense of the premartensitic domains, which can be recognized as first-order MT from premartensite to martensite. Typical martensitic image at 210 K is shown in Fig. 2(f). Therefore, the phase transition prior to MT can be verified as premartensitic transition.

Figure 3 shows the differential scanning calorimetry (DSC) curves for $Ni_{50}Mn_{34}In_{15.5}Al_{0.5}$ alloy upon cooling and heating at rete of 10 K/min. Large exothermic and endothermic peaks, corresponding to MT, premartensitic transition and their reverse transitions can be observed respectively. Thermal hysteresis clearly indicate the first-order nature of the two structural transitions. The Curie temperature of the martensite and austenite (T_C^M and T_C^A) can be identified as a distinct shoulder-like feature in the DSC curves, though the small endothermic peak is too weak to be observed upon heating around T_C^M. M_f obtained from of the $R(T)$ curves is a little higher than that obtained from DSC curves due to the influence of T_C^M. Except that, all the characteristic transition temperatures are relatively consistent.

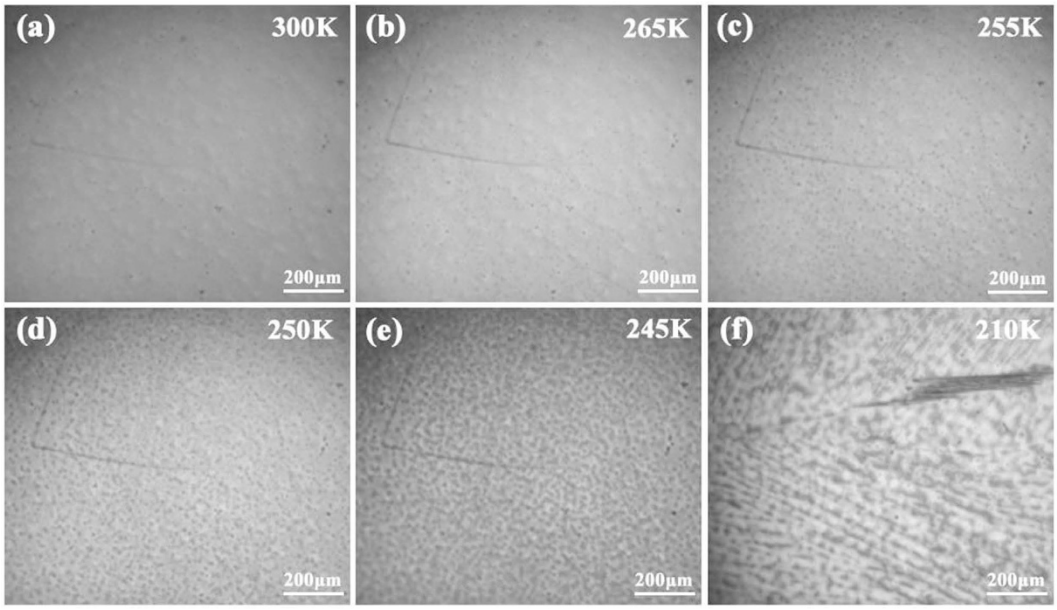

Figure 2. Optical micrographs at different temperatures for $Ni_{50}Mn_{34}In_{15.5}Al_{0.5}$ alloy upon cooling.

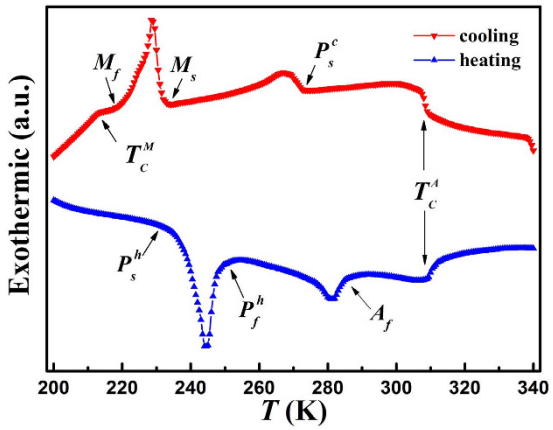

Figure 3. DSC curves for $Ni_{50}Mn_{34}In_{15.5}Al_{0.5}$ alloy upon cooling and heating.

Figure 4 shows temperature dependence of magnetization $M(T)$ curves measured upon cooling and heating processes with magnetic field of 100 Oe. All characteristic transition temperatures obtained from $M(T)$ curves are consistent with those obtained from DSC curves. Apart from the two ferromagnetic phase transition around T_C^M and T_C^A, the MT and premartensitic transition exhibit two successive magnetization jump from high magnetization state to weak magnetization state upon cooling. Obvious thermal hysteresis for both transitions confirms that each transition is first-order transition and they comprise two successive magneto-structural transitions. In Ni-Mn-Ga alloys, $M(T)$ curves exhibit two relative minimum-like anomaly kinks in quite narrow temperature interval with hardly detectable hysteresis far above MT, corresponding to premartensitic transition temperature T_p. However, in the present case, dc magnetization and ac susceptibility decrease P_s^h increase smoothly upon cooling/heating. Hence, it is clear that the premartensite appears around P_s^c in coexistence with the austenitic phase upon cooling. With further decrease of temperature, the austenitic phase fraction gradually decreases and approaches zero around M_s. Then the premartensite is transformed into martensite gradually from M_s to M_f. Similarly, on heating, the premartensite phase appears at, and the complete transition to premartensite phase occurs at P_f^h. Further increasing temperature result in the transition from premartensite to austenite until full austenite phase at A_f. In another word, the austenite and premartensite phases coexist between P_s^c and M_s upon cooling as well as between P_f^h and A_f upon heating. The magnitude of the magnetization difference across the premartensitic transition is about 30% of that across MT (while 12% for the inverse transition), while it is only about 2% in Ni-Mn-Ga, which indicates the enhanced magnetoelastic coupling in $Ni_{50}Mn_{34}In_{15.5}Al_{0.5}$ alloy at high temperature prior to MT. Reasonably, the chemical pressure induced by Al doping would be responsible for the appearance of the intermediate phase.

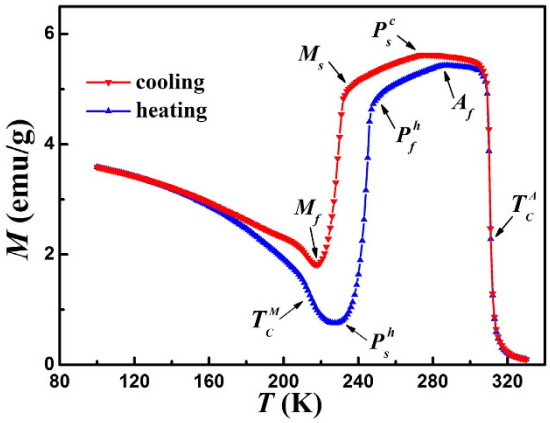

Figure 4. Temperature dependence of magnetization M (T) for the $Ni_{50}Mn_{34}In_{15.5}Al_{0.5}$ alloy measured upon cooling and heating with magnetic field of 100 Oe.

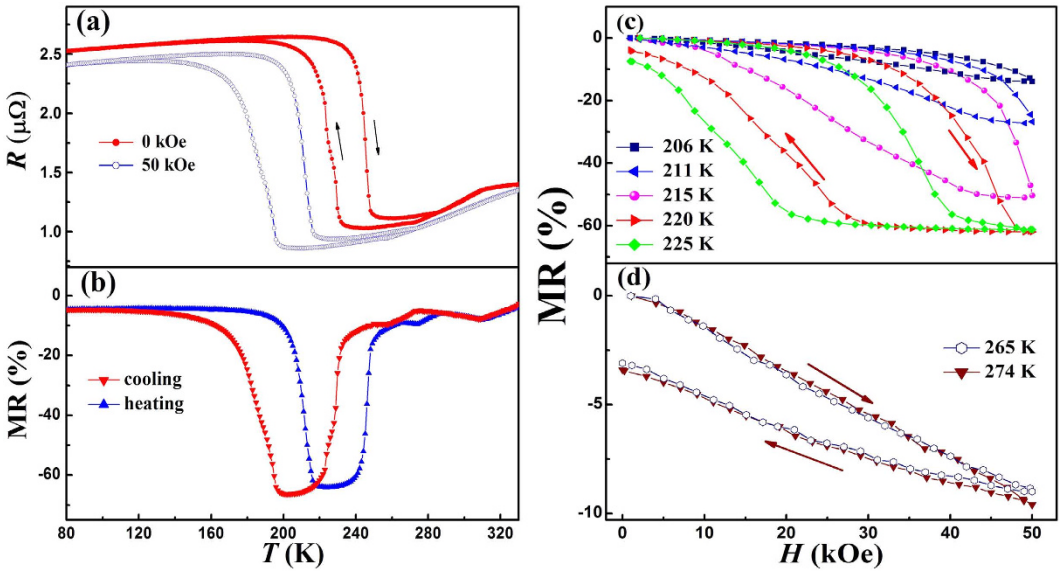

Figure 5. (**a**) Temperature dependence of resistance at 0 and 50 kOe for $Ni_{50}Mn_{34}In_{15.5x}Al_{0.5}$ alloy. (**b**) MR under a magnetic field of 50 kOe upon heating and cooling. (**c,d**) Field dependence of the MR at selected temperatures. Arrows indicate the direction of temperature and field variation.

With the large magnetization difference realized in the two successive magneto-structural transitions, we thus expect it to manifest a field-induced inverse transition. Figure 5(a) shows the temperature dependence of resistance $R(T)$ curves for $Ni_{50}Mn_{34}In_{15.5}Al_{0.5}$ alloy measured under zero field and 50 kOe. The R(T) curves under 50 kOe are found to be similar to that under zero field, but the phase transition temperatures notably shift to lower temperature under 50 kOe. The M_s is decreased by 34 K while P_s^c is decreased by 15 K. The large field dependences of transition temperatures can be attributed to the field-induced reverse MT, which further confirms that the two successive phase transitions originate from magnetoelastic coupling. Thus, large MR effects can be expected around the phase transitions. The MR was calculated as $(R_H\text{-}R_0)/R_0$, where R_H is the resistivity under magnetic field and R_0 is the resistivity at zero field. Figure 5(b) displays the temperature dependence of MR under 50 kOe. Upon heating, three negative peaks at 225 K, 274 K and 310 K with the value of 64%, 9.5%, and 8%, respectively, can be observed in the regions of MT, premartensitic transition and ferromagnetic-paramagnetic transition. The difference of MR upon cooling and heating in the regions of MT at low temperature is likely due to the different fractions of coexistent premartensite and martensite, as reported in conventional MT in the Ni-Mn based alloys. Similarly, the difference of MR upon cooling and heating in the regions of premartensitic transition at low temperature can be attributed to the different fractions of coexistent premartensite and austenite during premartensitic transition and the reverse one. In order to get a better understanding of the MR effects, isothermal MR curves are shown in increasing and decreasing magnetic fields at different temperatures, as described in inset of Fig. 5(c,d). For the measurements, firstly the samples were cooled down to 160 K from 340 K and then the temperature went up to the desirable temperature to perform magnetic field dependence of resistance. Between 205 K

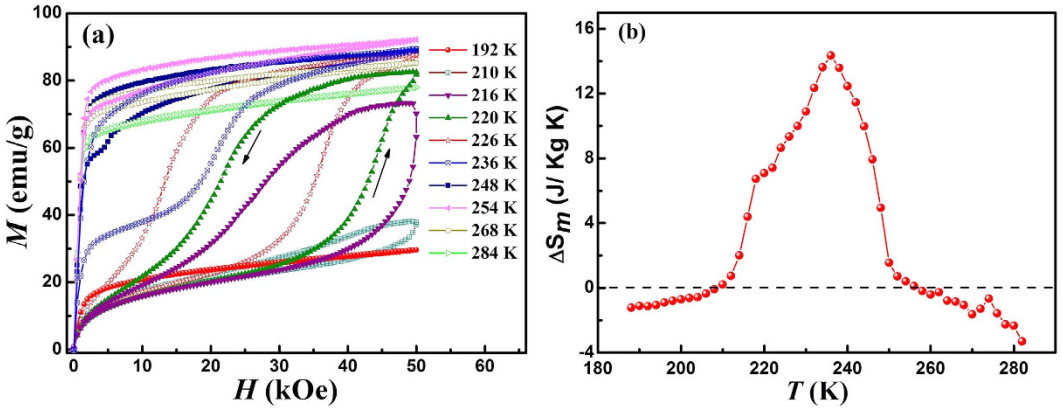

Figure 6. (**a**) Isothermal magnetization $M(H)$ curves for $Ni_{50}Mn_{34}In_{15.5}Al_{0.5}$ alloy at selected temperatures. (**b**) Temperature dependence of isothermal magnetic entropy change ΔS_m in the magnetic field of 50 kOe. Arrows indicate the direction of field variation.

and 225 K, the alloy is in the martensitic structure. Increasing magnetic field should induce the inverse MT from martensite to premartensite, and hence a sharp change in MR is observed in Fig. 5(c). The MR at low temperatures (205 K, 210 K and 215 K) can return to its original value of 0% after a field cycle up to 50 kOe, exhibiting a fully reversible behavior. However, the MR does not recover completely after a complete magnetization cycle at 220 K and 225 K. The magnitude of the irreversible MR increases with increasing temperature, indicating that the amount of remnant premartensite increase with temperature. This demonstrates that the magnetic field-induced austenite cannot be restored to martensite completely after demagnetization. At 265 K and 275 K, we get coexisting premartensite and austenitic phases in the sample. The magnetic-field-induced reverse premartensitic transition at the two temperatures can be indicated by the large magnetic hysteresis, shown in Fig. 5(d). The slow change of MR can be ascribed to the similar structure between the premartensite and austenite. Additionally, the irreversible behavior can observed, implying that the complete return transition (austenite to premartensite) cannot be realized.

The isothermal magnetization $M(H)$ curves at different temperatures with the field up to 50 kOe were measured, and the temperature step is 2 K. Figure 6(a) shows the typical M-H curves for the sample. Before each measurement, the sample was first cooled to 150 K (well below M_f) to ensure the same initial state of a fully transformed martensite and then heated to the measurement temperature. No visible hysteresis can be observed in the $M(H)$ curves at temperatures above 284 K (in the austenitic phase) and below 190 K (in the martensitic phase), which can be attributed to the absence of field-induced phase transition. The filed-induced transition from martensite to premartensite can be indicated by metamagnetic behavior and magnetic hysteresis between field-up and field-down processes. From Fig. 6(a), we can find that the premartensite start temperature under 50 kOe upon heating is at 220 K, which means application of 50 kOe can induce the complete transition from martensite to premartensite. Hence, with the increasing of austenite fraction at higher temperatures between 220 K and A_s (250 K), application of 50 kOe can not only induce transition from martensite to premartensite, but also induce transition from premartensite to austenite, which can be confirmed by the increasing of magnetization at 50 kOe from 220 K to 248 K, though there are no second metamagnetic behaviors. In accordance with the result of Fig. 5(d), the transition from premartensite to austenite can be displayed by the magnetic hysteresis in the representative curves at 254 K and 268 K.

The isothermal magnetic entropy change ΔS_m as a function of temperature and magnetic field can be calculated from magnetization isotherms using Maxwell relation $\Delta S_m = \int_{T_1}^{T_2} [\partial M/\partial T]_H dH$. Figure 6(b) shows the temperature dependence of ΔS_m in the magnetic field of 50 kOe. The spike-like behavior indicates the peak value (14.4 J/kg K) may be overestimated due to the application of Maxwell relation for first-order magnetostructural transition[37,38]. Nevertheless, such result can still be employed to study the origin of ΔS_m. In previous system with two successive magneto-structural transitions, either two-step MT[39] or MT and preceding intermediate phase transition[30], two positive ΔS_m peaks can be observed, corresponding to the two field-induced inverse phase transitions, respectively. In the present case, only one ΔS_m peak can be observed. According to the above analysis, the two-step inverse phase transition from martensite to premartensite, and then to austenite can be induced successively when applying magnetic field of 50 kOe at a constant temperatures between 220 K and 250 K. So both the two inverse phase transition induced by magnetic field contribute to the large value and wide temperature span of the peak, thus enhancing the magnetocaloric effect effectively.

Discussion

Premartensitic transition has been intensively investigated in Ni-Mn-Ga alloys for decades. However, owing to the small magnetization change and narrow temperature range across the premartensitic transition, the magnetic effects have seldom been reported. Since the occurrence of premartensitic transition in Ni-Mn-Ga alloys is a consequence of magnetoelastic coupling. The Ga-free Ni–Mn based FSMAs exhibit strong magnetoelastic coupling across MT, making them as excellent candidates to study the interesting properties associated with

premartensitic transition. Intermediate phase transition behaviors were observed in high-pressure annealing Ni–Mn–Co–Sn alloys, which can be attributed to the enhancement of magnetoelastic coupling at high temperatures prior to MT, while the enhancement of magnetoelastic coupling is resulted from the chemical pressure generated in the synthetizing process. Such chemical pressure can also be induced by smaller atom substitution. Here, in $Ni_{50}Mn_{34}In_{15.5}Al_{0.5}$ alloy formed by substituting In with smaller Al, pronounced premartensitic transition was detected by resistivity, *in situ* microscopic observation calorimetric and magnetic measurements, and the nature of first-order was displayed by thermal/ magnetic hysteresis. Our results indicate that smaller atom substitution would be an effective method to get more pronounced premartensitic transition behavior in Ni–Mn based FSMAs.

In summary, two successive magneto-structural transitions consisting of martensitic and premartensitic transitions were observed in $Ni_{50}Mn_{34}In_{15.5}Al_{0.5}$ alloy. The first-order nature of premartensitic transition can be evinced by microstructure evolution and large thermal/magnetic hysteresis. Owing to magnetoelastic coupling, the transitions temperatures shift to lower temperature with the external applied field. Large magnetoresistance and enhanced magnetic entropy change ΔS_m can be obtained associated with the field-induced inverse phase transitions.

Methods

The bulk $Ni_{50}Mn_{34}In_{15.5}Al_{0.5}$ alloy of nominal composition were prepared by arc-melting the required amount of constituent high purity (99.99% purity) elements in a cold copper crucible under argon atmosphere protection. An additional 2 wt.% Mn was added to compensate for evaporation losses. Homogenization was achieved by sealing the ingot under argon atmosphere in quartz ampoules and annealing at 1073 K for 24 h, followed by quenching in ice water. The sample used for imaging was polished and subsequently etched by dilute nitric acid. The *in situ* microscopic observation was performed using a magneto-optical imaging system (MOIS) attached with an ultrahigh speed camera. Heat flow data were collected by differential scanning calorimeter (DSC, Q2000, TA) on modulated mode with a cooling/heating rate of 10 K/min. The magnetic properties were measured by a superconducting quantum interference device (SQUID-VSM, Quantum Design) magnetometer and electrical transport properties were measured in a physical property measurement system (PPMS, Quantum Design).

References

1. Zheludev, A. *et al.* Phonon anomaly, central peak, and microstructures in Ni_2MnGa. *Phys. Rev. B* **51,** 11310–11314 (1995).
2. Kokorin V. V. *et al.* Pre-martensitic state in Ni–Mn–Ga alloys. *J. Phys.: Condens. Matter* **8,** 6457–6463 (1996).
3. Ma, Y. W., Awaji, S., Watanabe, K., Matsumoto, M. & Kobayashi, N. Effect of high magnetic field on the two-step martensitic-phase transition in Ni_2MnGa. *Appl. Phys. Lett.* **76,** 37–39 (2000).
4. Zheludev, A., Shapiro, S. M., Wochner P. & Tanner, L. E. Precursor effects and premartensitic transition in Ni_2MnGa. *Phys. Rev. B* **54,** 15045–15050 (1996).
5. Uijttewaal, M. A., Hickel, T., Neugebauer, J., Gruner, M. E. & Entel, P. Understanding the phase transitions of the Ni_2MnGa magnetic shape memory system from first principles. *Phys. Rev. Lett.* **102,** 035702 (2009).
6. Gonzàlez-Comas, A. *et al.* Premartensitic and martensitic phase transitions in ferromagnetic Ni_2MnGa. *Phys. Rev. B* **60,** 7085–7090 (1999).
7. Seiner, H., Kopecký, V., Landa, M. & Heczko, O. Elasticity and magnetism of Ni_2MnGa premartensitic tweed. *Phys. Status Solidi B* **251,** 2097–2103 (2014).
8. Cui, Y. T., Chen, J. L., Liu, G. D., Wu, G. H. & Wang, W. L. Characteristics of the premartensitic transition strain in ferromagnetic shape memory $Ni_{50.5}Mn_{24.5}Ga_{25}$ single crystals. *J. Phys.: Condens. Matter* **16,** 3061–3069 (2004).
9. Planes, A., Obradó, E., Gonzàlez-Comas, A. & Mañosa, L. Premartensitic transition driven by magnetoelastic interaction in bcc Ferromagnetic Ni_2MnGa. *Phys. Rev. Lett.* **79,** 3926–3929 (1997).
10. Opeil, C. P. *et al.* Combined Experimental and theoretical Investigation of the premartensitic transition in Ni_2MnGa. *Phys. Rev. Lett.* **100,** 165703 (2008).
11. Kim, J. H., Inaba, F., Fukuda, T. & Kakeshita, T. Effect of magnetic field on martensitic transition temperature in Ni–Mn–Ga ferromagnetic shape memory alloys. *Acta Mater.* **54,** 493–499 (2006).
12. Mañosa, L. *et al.* Phonon softening in Ni− Mn− Ga alloys. *Phys. Rev. B* **64,** 024305 (2001).
13. Barandiaran, J. M. *et al.* Magnetic field effect on premartensitic transition in Ni–Mn–Ga alloys. *Appl. Phys. Lett.* **94,** 051909 (2009).
14. Barandiarán, J. M. *et al.* Effect of martensitic transition and magnetic field on transport properties of Ni-Mn-Ga and Ni-Fe-Ga Heusler alloys. *Phys. Rev. B* **80,** 104404 (2009).
15. Zuo, F. *et al.* Magnetic and transport properties of the $Ni_{2-x}Mn_{1+x}Ga$ alloys. *J. Phys.: Condens. Matter* **11,** 2821–2830 (1999).
16. Wang, W. H. *et al.* Effect of low dc magnetic field on the premartensitic phase transition temperature of ferromagnetic Ni_2MnGa single crystals. *J. Phys.: Condens. Matter* **13,** 2607–2613 (2001).
17. Khovailo, V. V. *et al.* Premartensitic transition in $Ni_{2+x}Mn_{1-x}Ga$ Heusler Alloys. *J. Phys.: Condens. Matter* **13,** 9655–9662 (2001).
18. Zuo, F., Su, X. & Wu, K. H. Magnetic properties of the premartensitic transition in Ni_2MnGa alloys. *Phys. Rev. B* **58,** 11127–11130 (1998).
19. Ludwig, B. *et al.* Premartensitic transition in Ni_2MnGa Heusler alloys: Acoustic emission study. *Phys. Rev. B* **80,** 144102 (2009).
20. Singh, S., Bednarcik, J., Barman, S. R., Felser, C. & Pandey, D. Premartensite to martensite transition and its implications for the origin of modulation in Ni_2MnGa ferromagnetic shape-memory alloy. *Phys. Rev. B* **92,** 054112 (2015).
21. Sutou, Y. *et al.* Magnetic and martensitic transitions of NiMnX (X=In, Sn, Sb) ferromagnetic shape memory alloys. *Appl. Phys. Lett.* **85,** 4358–4360 (2004).
22. Kainuma, R. *et al.* Magnetic-field-induced shape recovery by reverse phase transition. *Nature* **439,** 957–960 (2006).
23. Krenke, T. *et al.* Inverse magnetocaloric effect in ferromagnetic Ni–Mn–Sn alloys. *Nature Mater.* **4,** 450–454 (2005).
24. Liu, J., Scheerbaum, N., Lyubina, J. & Gutfleisch O. Reversibility of magnetostructural transition and associated magnetocaloric effect in Ni–Mn–In–Co. *Appl. Phys. Lett.* **93,** 102512 (2008).
25. Sharma, V. K., Chattopadhyay, M. K. & Roy, S. B. Large magnetocaloric effect in $Ni_{50}Mn_{33.66}Cr_{0.34}In_{16}$ alloy. *J. Phys. D: Appl. Phys.* **43,** 225001 (2010).
26. Wang, R. L. *et al.* Effect of Al doping on the martensitic transition and magnetic entropy change in Ni–Mn–Sn alloys. *Solid State Comm.* **151,** 1196–1199 (2011).
27. Huang, L., Cong, D. Y., Suo, H. L. & Wang Y. D. Giant magnetic refrigeration capacity near room temperature in $Ni_{40}Co_{10}Mn_{40}Sn_{10}$ multifunctional alloy. *Appl. Phys. Lett.* **104,** 132407 (2014).

28. Yu, S. Y. *et al.* Large magnetoresistance in single-crystalline $Ni_{50}Mn_{50-x}In_x$ alloys (x=14–16) upon martensitic transition. *Appl. Phys. Lett.* **89,** 162503 (2006).
29. Chen, L. *et al.* Tuning martensitic transition and magnetoresistance effect by low temperature annealing in $Ni_{45}Co_5Mn_{36.6}In_{13.4}$ alloys. *J. Phys. D: Appl. Phys.* **44,** 085002 (2011).
30. Ma, S. C. *et al.* Investigation of the intermediate phase and magnetocaloric properties in high-pressure annealing Ni–Mn–Co–Sn alloy. *Appl. Phys. Lett.* **97,** 052506 (2010).
31. Ma, S. C. *et al.* Peculiarity of magnetoresistance in high pressure annealed Ni43Mn41Co5Sn11 alloy. *Appl. Phys. Lett.* **102,** 032407 (2013).
32. Xu, X., Ito, W., Katakura, I., Tokunagac M. & Kainuma, R. *In situ* optical microscopic observation of NiCoMnIn metamagnetic shape memory alloy under pulsed high magnetic field. *Scripta Mater.* **65,** 946–949 (2011).
33. Shen, Y. N. *et al.* Direct observation of magnetostructural transition in the Ni–Mn–Sn alloy using *in situ* optical microscope. *J Mater Sci: Mater Electron* **25,** 2030–2034 (2014).
34. Murakami, Y., Shibuya, H. & Shindo, D. Precursor effects of martensitic transformations in Ti-based alloys studied by electron microscopy with energy filtering. *J. Microsc.* **203,** 22–33 (2001).
35. Murakami, Y. & Shindo, D. Abstract Book of JIM Spring Meeting. *Narashino*. **350** (2001).
36. Otsuka, K. & Ren, X. Physical metallurgy of Ti–Ni-based shape memory alloys. *Prog. Mater. Sci.* **50,** 511–678 (2005).
37. Giguère, A. *at al.* Direct measurement of the "giant" adiabatic temperature change in $Gd_5Si_2Ge_2$. *Phys. Rev. Lett.* **83,** 2262 (1999).
38. Bourgault, D., Tillier, J., Courtois, P., Maillard, D. & Chaud, X. Large inverse magnetocaloric effect in $Ni_{45}Co_5Mn_{37.5}In_{12.5}$ single crystal above 300K. *Appl. Phys. Lett.* **96,** 132501 (2010).
39. Li, Z. *et al.* Two successive magneto-structural transitions and their relation to enhanced magnetocaloric effect for $Ni_{55.8}Mn_{18.1}Ga_{26.1}$ Heusler alloy. *Sci. Rep.* **5,** 15143 (2015).

Acknowledgements

The authors thank National Natural Science Foundation of China (Grant No. 11104065, 11547191 and 51402094), Postdoctoral Science Foundation of China (Grant No. 2013M542008), Hubei Provincial Department of Education (Grant No. Q20120108 and Q20141004), and Hubei Provincial Department of Science & Technology (Grant No. 2015CFB549 and 2015CFB397) for their financial supports.

Author Contributions

R.L.W. and C.P.Y. conceived and designed the experiments. S.Y.Y. and Y.Q.W. prepared the sample. Y.Q.W. and S.P.G. performed the magnetic measurements and prepared the figures. Y.Q.W. and Y.L. performed the electrical transport measurements. H.C. and Z.C.X. performed the *in situ* optical microscopic observation. H.B.X., L.F.X. and R.X. contributed to the discussion of the results. R.L.W. wrote the paper. All the authors reviewed the manuscript.

Additional Information

Competing financial interests: The authors declare no competing financial interests.

How to cite this article: Wu, Y.Q. *et al.* Premartensitic transition and relevant magnetic effects in $Ni_{50}Mn_{34}In_{15.5}Al_{0.5}$ alloy. *Sci. Rep.* **6**, 26068; doi: 10.1038/srep26068 (2016).